Studia Quaternaria, vol. 37, no. 2 (2020): 91–99 DOI: 10.24425/sq.2020.133753

HOLOCENE CLIMATE DYNAMICS IN SUMBA STRAIT, INDONESIA: A PRELIMINARY EVIDENCE FROM HIGH RESOLUTION GEOCHEMICAL RECORDS AND PLANKTONIC FORAMINIFERA

Purna Sulastya Putra*, Septriono Hari Nugroho

Research Center for Geotechnology LIPI, Kompleks LIPI Gd 80, Jalan Sangkuriang Bandung 40135 Indonesia; e-mail: purna.putra@gmail.com

** corresponding author*

Abstract:
The dynamics of climatic conditions during the Holocene in the Sumba Strait is not well known, compared with in the Indian Ocean. The aim of this paper is to identify the possible Holocene climate dynamics in Sumba Strait, eastern Indonesia by using deep-sea core sediments. A 243 cm core was taken aboard RV Baruna Jaya VIII during the Ekspedisi Widya Nusantara 2016 cruise. The core was analyzed for elemental, carbonate and organic matter content, and abundance of foraminifera. Based on geochemical and foraminifera data, we were able to identify at least six climatic changes during the Holocene in the Sumba Strait. By using the elemental ratio of terrigenous input parameter, we infer to interpret that the precipitation in the Sumba Strait during the Early Holocene was relatively higher compared with the Mid to Late Holocene.

sq

Key words: climate dynamics, planktonic foraminifera, Holocene deep-sea sediment, Sumba Strait

Manuscript received 20 September 2019, accepted 9 March 2020

INTRODUCTION

Global mean surface temperature warmed by 0.85°C between 1880 and 2012, as reported in the IPCC Fifth Assessment Report (IPCC, 2013). Many regions of the world with 20–40% of the global population have already greater regional-scale warming (depending on the temperature dataset used) having experienced over 1.5°C of warming in at least one season (IPCC, 2017). Temperature rise has already resulted in profound alterations to human and natural systems, including increases in droughts, floods, and some other types of extreme weather; sea level rise; and biodiversity loss – these changes are causing unprecedented risks to vulnerable persons and populations (IPCC, 2012, 2014). Among the significant attempts for understanding temperature changes is the study of the Holocene climate dynamics. For example in Cambodia, Maxwell (1999) identified the Last Glacial Maximum period terminated about 8500 BP, which is more that 1000 years later compared with southwestern China. Park *et al.* (2019) identified 9 dry events during the Holocene in the southern sea-coast region of Korea. On the other hand, Kuhnert *et al.* (2014) identified that the most dramatic change during the Holocene was the temperature drop by up to 2°C leading toward the cool interval between 5,600 to 4,200 BP.

The Holocene climatic changes were recorded in the Sumba region, eastern Indonesia (Ardi, 2018). However, most of the palaeoclimate reconstructions in this region and adjacent area were based on coral data (e.g. Gagan *et al.*, 1998; Gagan *et al.*, 2000; Watanabe *et al.*, 2003), with very few studies only that used deep-sea sediments. It is very important to study the palaeoclimate dynamics by using deep-sea sediments, because a climate response in the corals and sediments may be different. Some examples of these few deep-sea core studies are Steinke *et al.* (2014), Liu *et al.* (2015) and Ardi (2018). Steinke *et al.* (2014) used deep-sea sediments taken from the northwestern Sumba Island to identify the upwelling variability off southern Indonesia based on shell Mg/Ca of the planktonic foraminiferal species. On the other hand, Liu *et al.* (2015) used deep-sea sediments collected to the south of the Sumba Island to reconstruct dust contributions from the Australian continent and volcanic eruptions history over the last 300,000 years in the region. Ardi (2018) used planktonic foraminifera assemblage to reconstruct the palaeoclimate and palaeoceanographical conditions from the Late Pleistocene in the southern off Sumba Island. Our paper aims to fill the gap by examining deep-sea sediments taken from the Sumba Strait to identify the possible Holocene climate dynamics.

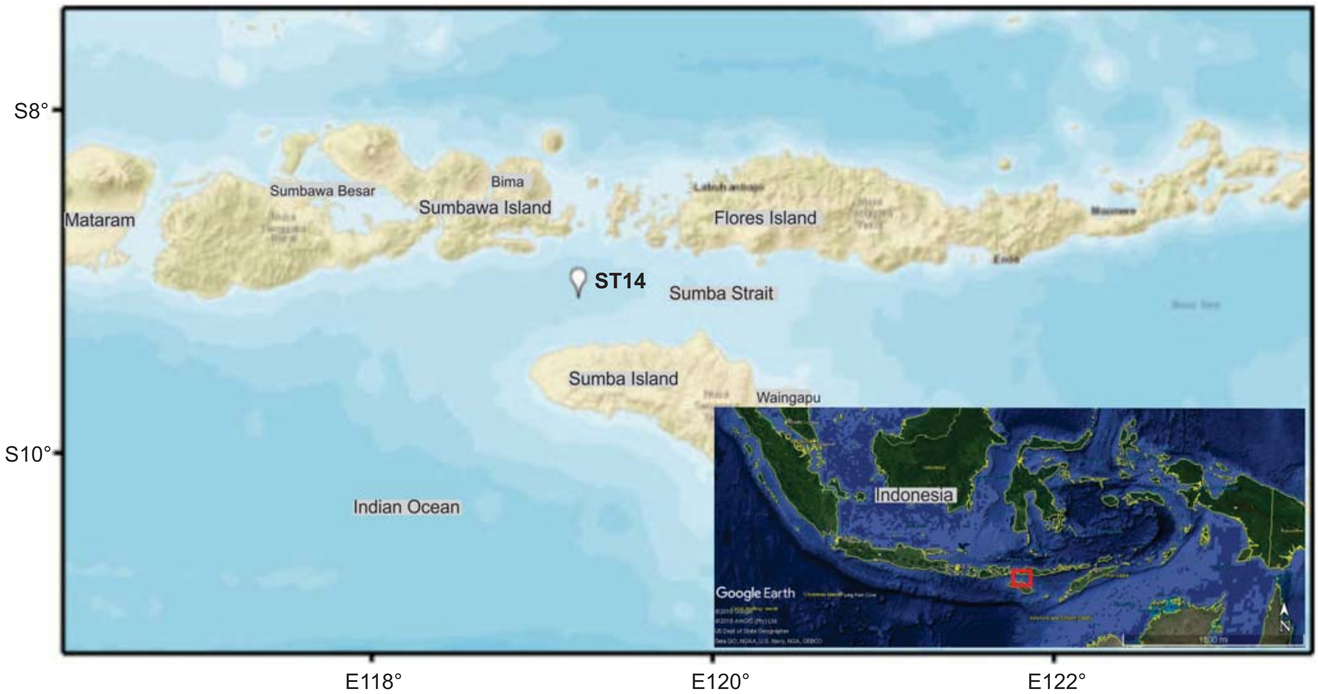

Fig. 1. Location of the studied site. The ST 14 core located in the Sumba Strait, Nusa Tenggara, Indonesia.

As a preliminary study, this research will be focused on a relatively practical data based on the planktonic foraminifera assemblages, elemental analysis as well as organic matter and carbonate content. Planktonic foraminifera assemblages is one of the foraminiferal proxies that can be used to reconstruct the palaeoclimates conditions (Saraswat, 2015). Based on Chauhan *et al.* (2013) the dynamics of organic matter and carbonate content within deep-sea sediments can be used to reconstruct the past climatic variations. We also identify the possible rainfall variability during the Holocene based on elemental ratio. According to Gustiantini (2018), Fe, Ti, and Rb are elements which might reflect a terrigenous input. Those elements then normalized against Ca which assumed to be mainly derived from marine shells (Langer, 2008).

METHODS

In this section we will describe the detail of the methodology and approaches that used for this study. The Holocene climate change in the Sumba Strait was reconstructed by using geochemical records (elemental analysis and loss on ignition/LoI analysis) and planktonic foraminifera data of the deep-sea sediments. A 243 cm long core (ST 14 core) was used and all analyses were completed at the Research Center for Geotechnology, Indonesian Institute of Sciences (LIPI) in Bandung, Indonesia. The core was taken from the Sumba Strait, eastern Indonesia from the depth of 1283 m, using a gravity corer on board of Baruna Jaya VIII Research Vessel during the Ekspedisi Widya Nusantara 2016 cruise. ST 14 was the longest core obtained from the Sumba Strait during the cruise. Samples were collected at every 5 cm interval along the core and a total of 48 samples were used for this study. The survey site is located at the coordinates of 119°12’849” E and 09°05’082” S (Fig. 1).

Approximately 5 grams of sediments per sample used for foraminifera analysis. As the samples were loose, foraminifera analysis using the swirling method without hydrogen peroxide was applied. This swirling method used to separate the foraminifera from the mud. Planktonic foraminifera is well known as one of the best proxy for palaeoenvironment (palaeoclimate and palaeocenographic) reconstruction due to its environmental change sensitivty, especially during the Quaternary (Sijinkumar and Nath, 2012). Ardi (2018) proved the effectiveness of this proxy to reconstruct the palaeoclimatic and palaeoceanographic conditions off the Sumba Island.

Loss on ignition (LoI) analysis is used to obtain the organic and carbonate content in the sediment. The LoI analysis following the method of Robertson (2011). At first, samples were burnt at 105°C for 4 hours to eliminate the water content. To calculate the organic matter, samples were burnt at 550°C for 4 hours. After that, the samples were burnt again at 1050°C for 2 hours to calculate a carbonate content. Weight difference after and before burning both at 550°C and 1050°C reflected losses of organic matter and carbonate content, respectively. Chauhan *et al.* (2013) identified that drops of organic matter corresponding with rise of carbonate content in deep-sea sediments could be referred to warm and humid conditions, and vice versa.

Table 1. The concentration of elements (Rb, Ti, Fe and Ca) and the elemental ratios in the core.

Depth (cm)	Ca ppm	Ti ppm	Fe ppm	Rb ppm	Ln(Fe/Ca)	Ln(Ti/Ca)	Ln(Rb/Ca)	Period
0	86589.26	767.87	7565.94	16.15	-2.43752	-4.72531	-8.58701	Holocene
5	125716.31	869.34	7606.21	11.11	-2.80506	-4.97405	-9.33394	
10	106117.22	624.03	5427.74	11.97	-2.97302	-5.13610	-9.08990	
15	108296.18	887.18	8351.48	7.96	-2.56243	-4.80458	-9.51820	
20	112469.93	701.14	6833.46	9.97	-2.80085	-5.07773	-9.33086	
25	100904.84	879.28	7183.67	15.79	-2.64237	-4.74283	-8.76256	
30	102979.91	905.09	6120.15	9.41	-2.82295	-4.73425	-9.30052	
35	97941.12	1008.36	6899.04	16.99	-2.65298	-4.57604	-8.65950	
40	109252.72	865.57	7585.75	17.87	-2.66739	-4.83803	-8.71830	
45	124674.85	701.35	6135.72	12.06	-3.01158	-5.18046	-9.24357	
50	108363.83	726.85	6147.77	13.79	-2.86940	-5.00453	-8.96931	
55	112818.92	869.09	6319.38	18.57	-2.88216	-4.86609	-8.71199	
60	103921.45	1088.03	6616.81	12.16	-2.75402	-4.55927	-9.05324	
65	107991.73	787.64	6888.81	11.22	-2.75216	-4.92077	-9.17211	
70	108051.81	939.87	6941.17	14.42	-2.74514	-4.74462	-8.92175	
75	123146.32	813.84	5808.90	12.70	-3.05398	-5.01936	-9.17953	
80	102377.39	938.64	6060.61	13.00	-2.82686	-4.69199	-8.97147	
85	84071.62	950.02	7058.35	15.05	-2.47746	-4.48294	-8.62805	
90	139829.45	812.82	6301.23	14.06	-3.09968	-5.14767	-9.20484	
95	99437.21	1150.68	6860.26	13.79	-2.67378	-4.45917	-8.88334	
100	90107.23	1112.36	7129.44	13.36	-2.53677	-4.39452	-8.81649	
105	81631.58	1225.23	7839.98	15.94	-2.34298	-4.19909	-8.54114	
110	73118.35	1015.21	6381.21	14.03	-2.43872	-4.27698	-8.55864	
115	85007.55	914.82	6589.68	16.51	-2.55724	-4.53177	-8.54653	
120	72066.38	821.10	6201.34	15.47	-2.45282	-4.47470	-8.44644	
125	62922.57	812.14	6221.21	16.41	-2.31394	-4.34999	-8.25177	
130	89039.67	986.37	6764.57	15.77	-2.57738	-4.50281	-8.63873	
135	88147.98	1205.84	6970.52	14.42	-2.53733	-4.29184	-8.71816	
140	81695.55	1076.70	6599.31	16.04	-2.51603	-4.32910	-8.53567	
145	79184.34	993.99	5847.12	13.86	-2.60583	-4.37781	-8.65053	
150	82937.45	988.96	6127.58	15.79	-2.60529	-4.42919	-8.56647	
155	82992.16	1156.55	7077.86	16.43	-2.46177	-4.27330	-8.52739	
160	76699.52	999.39	6958.31	18.97	-2.39996	-4.34051	-8.30479	Pleistocene
165	92358.76	879.31	5458.33	15.89	-2.82854	-4.65430	-8.66775	
170	80006.63	964.68	5823.09	15.28	-2.62028	-4.41807	-8.56332	
175	74124.16	1119.39	6201.68	17.94	-2.48092	-4.19296	-8.32646	
180	71721.90	1162.77	5616.98	13.68	-2.54700	-4.12199	-8.56462	
185	73678.21	1029.77	6439.47	12.94	-2.43726	-4.27037	-8.64714	
190	78430.17	1238.10	7188.37	15.15	-2.38974	-4.14863	-8.55196	
195	78010.18	1141.71	6236.05	14.68	-2.52649	-4.22431	-8.57811	
200	78452.06	962.44	6376.40	10.89	-2.50988	-4.40077	-8.88240	
205	82471.87	892.89	5833.87	15.32	-2.64878	-4.52575	-8.59105	
210	87586.59	1001.95	6170.06	16.54	-2.65292	-4.47068	-8.57460	
215	92546.70	945.92	6312.87	13.21	-2.68512	-4.58331	-8.85449	
220	87302.58	942.00	5792.47	15.06	-2.71282	-4.52913	-8.66509	
225	94771.02	828.77	5561.09	16.75	-2.83567	-4.73928	-8.64082	
230	86880.54	1187.44	6558.19	16.66	-2.58382	-4.29273	-8.55928	
235	78354.49	1072.09	5828.71	15.67	-2.59845	-4.29163	-8.51725	
240	83526.00	1089.96	7269.94	18.29	-2.44141	-4.33902	-8.42656	

The samples scanned using Thermo NITON XL3t 500 scanner to obtain the elemental composition. The main advantage of XRF is that element intensities are obtained directly by scanning the core sediment surface without any destruction or extraction like found in conventional geochemical methods (Weltje and Tjalingii, 2008). Fe, Ti, and Rb are elements, intensity of which might be related to the terrigenous input (Steinke *et al.*, 2014; Gustiantini, 2018). Fe and Ti could be derived from mafic minerals contained in mafic and ultramafic rocks composing the adjacent island

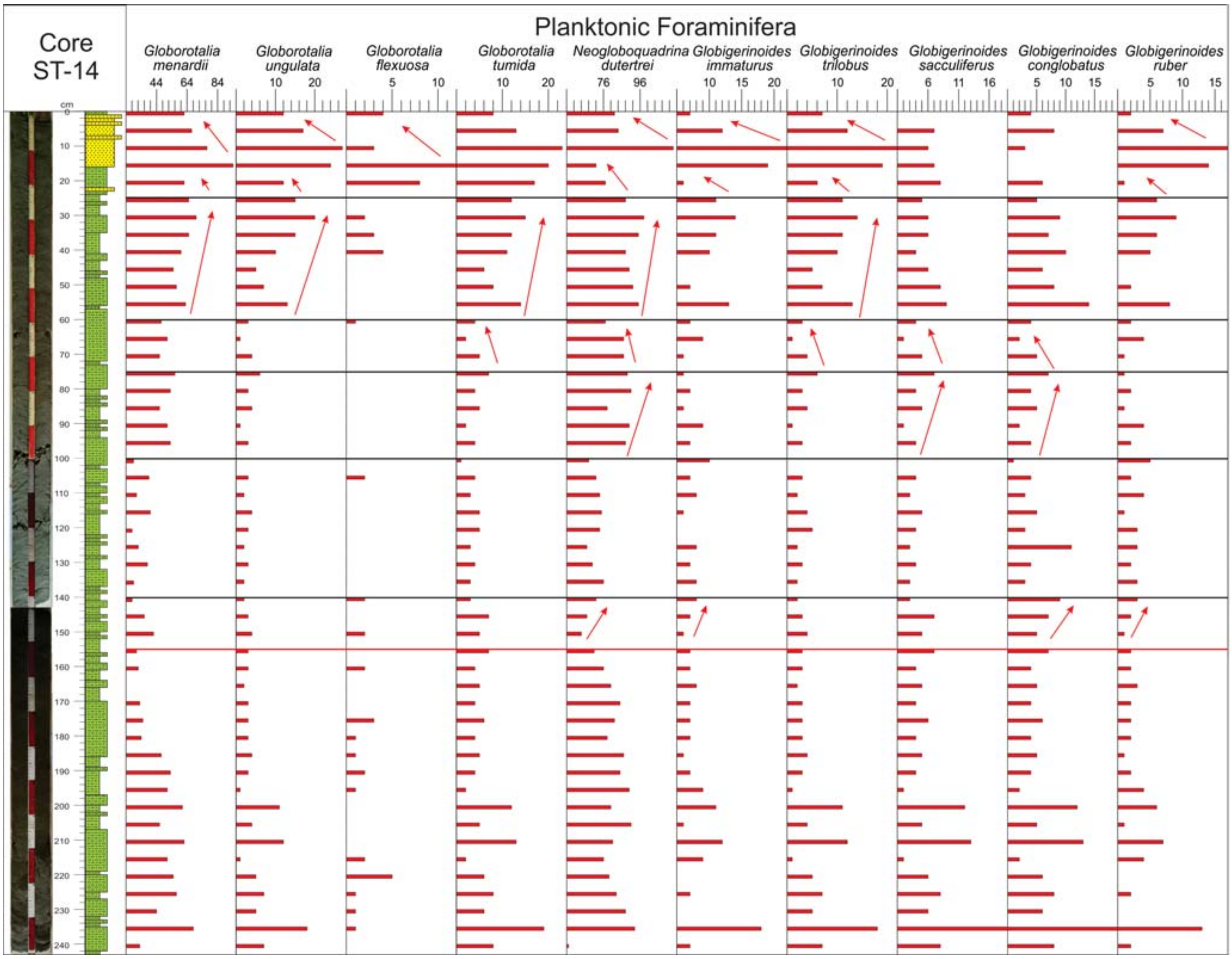

Fig. 2. The dynamics of the Holocene climatic variation based on LoI and foraminiferal abundance data. Horizontal red line is the boundary of Pleistocene/Holocene, black line is the boundary of each past climatic change. Red arrow indicates rises or drops in organic matter, carbonate content and foraminifera abundance.

(Kissel *et al*., 2010). On the other hand, Rb is associated with fine grained siliceous clastic sediments including clay minerals from the adjacent island (Dypvik and Harris, 2001). These elements were then normalized against Ca which assumed to be mainly derived from marine shells, indicating a prominent marine origin (Langer, 2008; Gustiantini, 2018).

RESULTS

Foraminifera Content

A total of 17 planktonic foraminifera species were identified in the core ST 14 (Fig. 2). At first we used the occurrence of some planktonic foraminifera species to identify the Pleistocene/Holocene boundary. *Globigerina calida calida* is one of the Holocene type species (Blow, 1969). This species was used to identify the Holocene sediment in the core. The Holocene was indicated by the first occurrence of *Globigerina calida calida*. it means that the boundary Pleistocene/Holocene is located at depth of approximately 156 cm (Fig. 2). The other foraminifera species were distributed along the core. In general, most species of Globorotalia, along with *Globigerinoides imaturus*, *Globigerinoides ruber* and *Hastigerina aequilateralis* were abundant in the lower and upper part, and decreased in the middle part of the core. This trend is different for *Globoraotalia flexuosa* that is relatively abundant in the upper part of the core only. *Globigerinoides sacculiferus* prevails in the lower part of the core. *Neogloboqaudrina dutertei* was the most abundant species along the core. On the other hand, *Orbulina universa* was identified mostly in the middle part of the core.

Carbonate and Organic Matter Content

The loss on ignition (LoI) presents the organic matter and carbonate content in the deep-sea sediments is presented (Fig. 2). During the Pleistocene, the organic matter content was generally increasing (with some fluctuations)

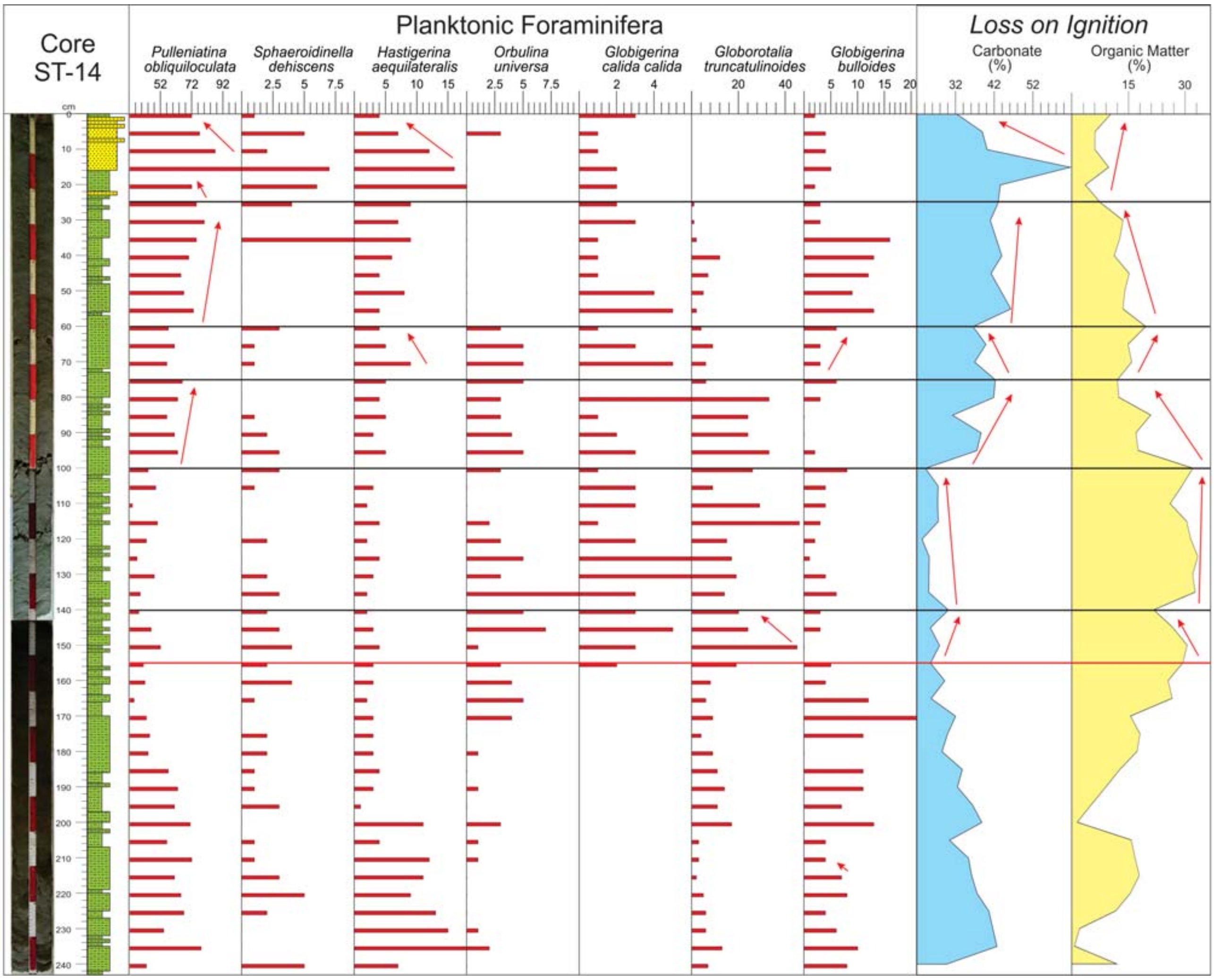

Fig. 2. *continued.*

from 10.25% at the bottom to 18.88% at the boundary Pleistocene/Holocene. On the other hand, the carbonate content decreases from 42.67% at the bottom to 25.68% at the end of the Pleistocene. The carbonate content was increasing from 23.32% in the Early Holocene to 61.64% in the upper part of the core, parallel to a decreasing content of organic matter from 21.14% to 11.19%. A peak of carbonate content occured at 14 cm depth (Fig. 2).

Terrigenous Input Parameter

The curve of terrigenous input of elemental ratio of Rb/Ca, Ti/Ca and Fe/Ca indicates a relatively similar pattern (Fig. 3). In general, the ratio is higher during the Pleistocene than in the Holocene. It is related to higher value of Rb and Ti during the Pleistocene (Table 1). The average of Rb and Ti content in the Pleistocene sediment are 15.47 ppm and 1026.98 ppm, while 14.13 ppm and 924.87 ppm in the Holocene, respectively. The Fe content in the Pleistocene is slightly lower (6213.29 ppm) compared with the Holocene (6771.86 ppm).

DISCUSSION

During the Holocene, 6 climatic periods could be distinguished. Although there is no dating available in this preliminary study, 6 periods of the Holocene climate change were distinguished are in agreement with other studies of the tropical areas. Mayewski *et al.* (2004) identified that globally there were 6 climatic phases during the Holocene that are characterized by polar cooling, tropical aridity and major atmospheric circulation changes. Recently, this 6 climatic changes during the Holocene were put together into 3 stages by Walker *et al.* (2019). The dynamic of climatic variation based on the organic matter and carbonate content and foraminifera abundance is presented (Fig. 2).

Temperature Changes

Boltovskoy and Wright (1976) divided the foraminiferal assemblage of equatorial to South Pacific into 5 zones based on sea surface temperature. Those 5 foraminiferal assemblage zones are: species that are widely distributed (tem-

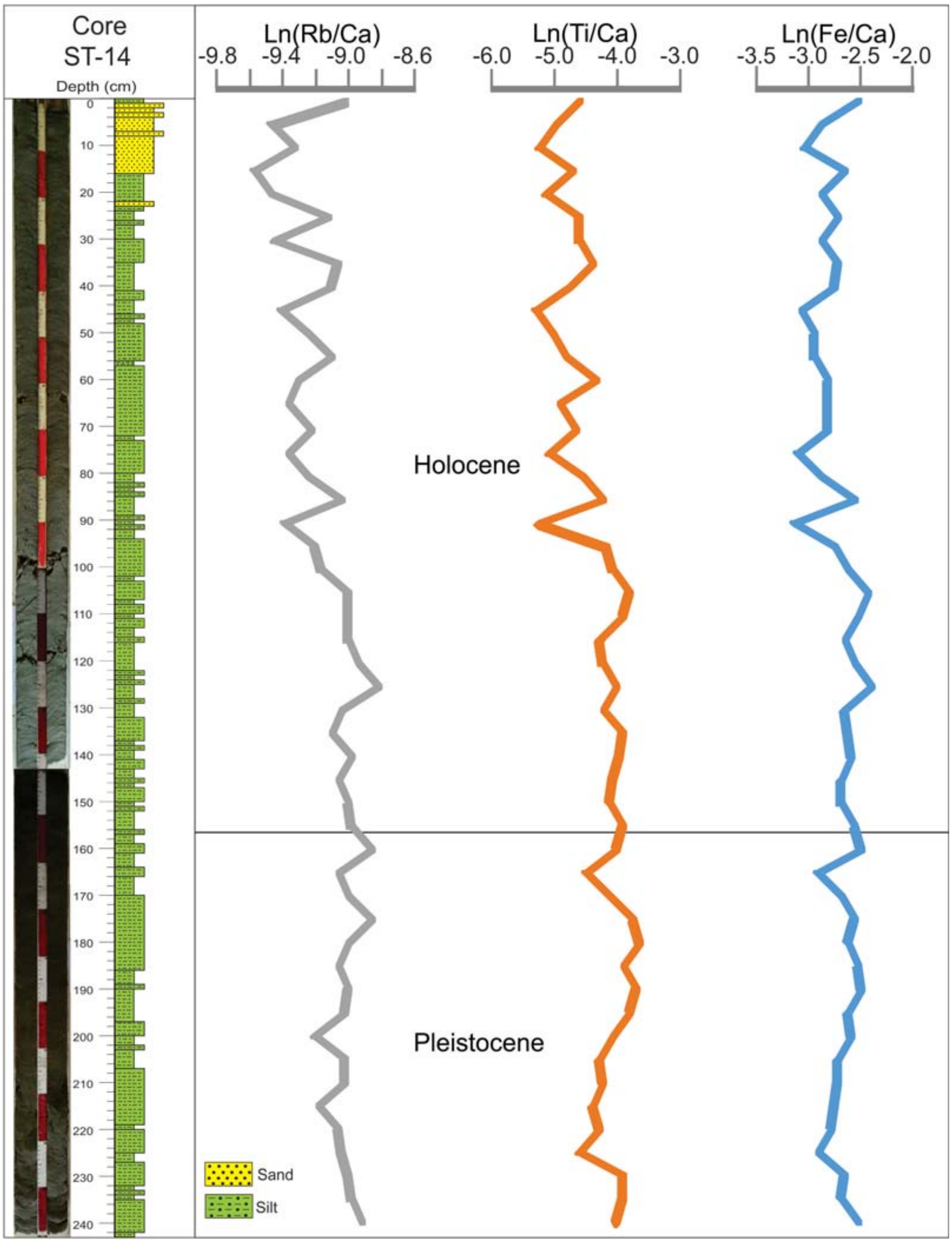

Fig. 3. The elemental ratio of terrigenous input proxies (Rb/Ca, Ti/Ca and Fe/Ca) obtained from the XRF analysis.

perature of 9–27.6°C) include *Globigerinella aequilateralis*, *Globigerinoides ruber*, *Hastigerina pelagica* and *Orbulina universa*, equatorial species with temperature of 16–28°C with *Globigerinoides conglobatus*, *Globigerinoides sacculiferus* and *Globigerinoides eggeri*, equatorial species (temperature of 24–28°C) comprised of *Globigerina conglomerate*, *Globigerina hexagona*, *Globorotalia menardii* and *Pulleniatina obliqueloculata*. Middle subantric species (temperature of 9–24°C) include *Globigerina bulloides*, *Globigerina inflata*, *Globorotalia punctulata* and *Globorotalia truncatulinoides*, and subantric species with temperature of 9.2–11.5°C that comprised *Globorotalia scitula*. This foraminiferal assemblage zonation is applied in our core and some species are correlated well.

Pleistocene

The occurrence of *Globigerina bulloides* that reflected a cold condition was highly abundant in the Pleistocene sediment compared with the Holocene sediment. On the other hand, *Globigerina minardii* as equatorial species (re-

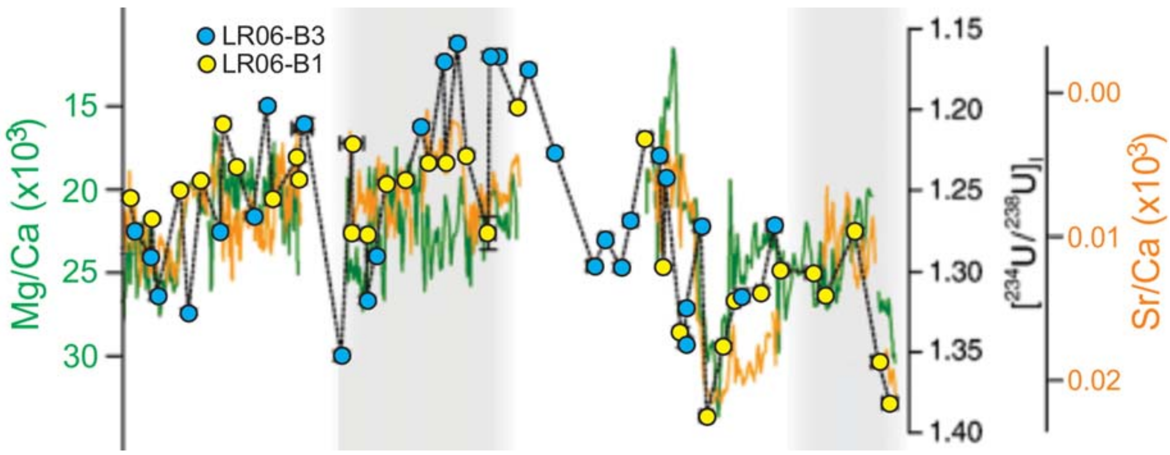

Fig. 4. The observed higher $^{234}U/^{238}U$ values during the Early Holocene (12.6 ka to -9.5 ka) are consistent with results of the trace element analysis(Sr/Ca and Mg/Ca value), indicating reduced precipitation and dissolution rates (Griffiths *et al.*, 2010).

flecting warmer condition) was increased from the beginning of Holocene (Fig. 2). In general, the Late Pleistocene was characterized by the drop of carbonate content with an increases of organic matter that reflecting a relatively cold and dry conditions.

Early Holocene

A climatic variation in the Early Holocene (depth 140–155 cm) was characterized by higher carbonate content with a drop of organic matter (Fig. 2), reflecting relatively warm and humid conditions. Chauhan *et al*. (2013) indicate that such conditions were characterized by increased of carbonate content. This warm and humid conditions in the Early Holocene are observed globally (Bryson *et al*., 1969; Setiabudi, 1985). This period was also reflected by the abundance trend of some planktonic foraminifera species, for example increase of *Globigerinoides conglobatus*, an equatorial type (warm) species. An increases in abundance of some other species was also observed, for example of *Neogloboquadrina dutretrei* and *Globigerinoides sacculiferus*. Contents of some typical species of cold conditions (subantric species) decreased, for example of *Globorotalia truncatulinoides*.

Middle Holocene

The next climatic phase observed in the studied core occurred at 100–140 cm depth (Fig. 2) and was characterized by the relatively lower value of carbonate content and relatively higher value of organic matter compared with the Early Holocene and it reflected cold and dry conditions according to Chauhan *et al*. (2013). We interpreted that the global 8.2 ka cooling event (Ellison *et al*., 2006; Burger, 2010) is recorded at this depth interval, with foraminifera less abundant compared with the upper part of the core. Some species e.g *Globigerina bulloides* were more common.

The next climatic change in the Middle Holocene was indicated by relatively stable contents of most foraminifera species. There was a sudden increases in carbonate content and drop of organic matter at depth 100–75 cm. We interpret that the global event of the Middle Holocene climatic optimum is observed at this depth.

Late Holocene

This period was characterized by decreased carbonate content and a rise in organic matter, reflecting relatively cold and dry conditions. Some planktonic foraminifera species are more abundant, for example *Globorotali menardii*, *G. tumida* and *Globigerinoides ruber.* There is a peak of carbonate content at depth of 15 cm. We interpreted this as a response of the Medieval Warm Period, that occurred around 900–1300 AD (Keigwin, 1996; Easterbrook, 2016). Easterbrook (2016) however indicated that this Medieval Warm Period was mostly recorded in Europe. Detailed analysis is important to provide a more precise interpretation of this carbonate content peak. This peak was correlated with the peak of some species content, for example of *Globorotali menardii*, *G. tumida*, *G. flexuosa*, *Neogloboquadrina dutertei* and *Globigerinoides ruber.* This peak was then followed by a decrease of carbonate content and some equatorial species, for example *Globorotali menardii*, which indicated an abrupt temperature drop related to the Little Ice Age (Bradley and Jonest, 1993).

Precipitation Changes

The elemental ratio proxies for terrigenous input (Fe/Ca, Ti/Ca and Rb/Ca) were used to infer rainfall variability off the Sumba Strait since the Early Holocene (Fig. 3). We infer that the elements identified in our deep-sea sediments were derived from the Sumba Island and the Sumbawa Island, located to the south and north of our survey area, respectively. Effendi and Appandi (1993) and Lytwyn *et al.* (2001) identified that besides carbonate rocks, both on the Sumbawa Island and the Sumba Island, they are composed of Cretaceous to Holocene volcanic and volcanoclastic rocks.

Elemental ratio proxies which have the capability to infer past rainfall conditions from terrigenous input have been proven as an effective practical method (Dypvik and Harris, 2001; Hemming, 2007; Kissel *et al.*, 2010). In general, larger elemental ratio indicates higher terrigenous intensity that reflects rainfall intensity. The elemental ratio was slightly higher in the Early to Middle Holocene compared to those in the Late Holocene (Fig. 3). It means that the rainfall intensity recorded in our deep-sea sediment was slightly higher during the Early Holocene compared with the Late Holocene. This result is different from other studies that prove a decreased rainfall intensity in the Early Holocene as observed in southern Java (Mohtadi *et al.*, 2011) and Flores offshore (Fig. 4, Griffiths *et al.*, 2010). In this preliminary study the main factors responsible for the rainfall intensity were not identified, however the rainfall pattern in the Late Holocene is relatively similar in our and other studies in southern Java and Flores offshore where the rainfall intensity increased.

CONCLUDING REMARKS

Based on geochemical data (organic matter and carbonate content) and foraminiferal data, the climatic change during the Holocene was identified by at least 6 climatic phases, reflected by the repeated warm-humid and cold-dry conditions. This result is consistent with other studies of the tropical area (Kalimantan by Yulianto, 2001). Yulianto (2001) identified that during the Early Holocene, the climatic was relatively warm and humid. On the other hand, there was an anomaly of climatic conditions during the Early Holocene in the tropical area, that showed unusually cold conditions, probably caused by high concentration of dust as observed by Ruddiman and Mix (1993) in the tropical South Atlantic Ocean and by Thompson *et al.* (1995) in the central Andes.

Based on the elemental ratio as the index of terrigenous input, the rainfall condition during the Early Holocene was relatively higher compared with the Mid–Late Holocene. Griffiths *et al.* (2009) suggested that intensification of the monsoon rainfall was driven by sea level rise that increased moisture supply to the Indonesian Archipelago. The sea level rise then managed to drown the Java Sea and Karimata Strait, made warmer water flow eastwards (Linsley *et al.*, 2010). According to Griffiths *et al.* (2009) and Ding *et al.* (2013) the presence of warmer surface water increased the overall sea surface temperature and could be related to the enhanced rainfall.

More detailed studies are needed to provide more precise climate changes in the Holocene. However, this preliminary study proves that simple and practical methods of geochemical and foraminifera analysis from the deep-sea sediments provide some early and important insights on Holocene climate dynamics in Sunda Strait, Indonesia.

Acknowledgments

We are grateful to the captain and crew of RV Baruna Jaya VIII and to Dr Udhi Hernawan as the Ekspedisi Widya Nusantara 2016 coordinator. The cruise was funded by Research Center for Oceanography, Indonesian Institute of Sciences (LIPI). We would like to thanks Jakah and Ahmad N for helping us with the laboratory analysis. This manuscript benefited from the constructive and helpful comments and suggestions from the reviewer and editor.

Authors' Contribution

PSP is the main author of this paper. PSP and SHN joined the cruise, collected the samples and analyzed the samples. PSP wrote the initial draft of the manuscript. Both authors read and approved the final manuscript.

REFERENCES

Ardi, R.D.W., 2018. Palaeoclimatology and palaeo-oceanography reconstruction since Late Pleistocene based on foraminiferal assemblages off the southwest coast of Sumba Island, East Nusa Tenggara. Master Thesis, Institut Teknologi Bandung (in Indonesian with English summary).

Blow, W.H., 1969. Late Middle Eocene to Recent planktonic foraminiferal biostratigraphy. Proceedings of the first international conference on planktonic microfossils 1, 199–422.

Boltovskoy, E., Wright, R., 1976. Planktonic foraminifera. In: Boltovskoy, E., Wright, R. (Eds), Recent Foraminifera, 166–189, Springer, Dordrecht.

Burger, M., 2010. The effects of the 8.2 ka event on the ITCZ in the tropical Atlantic. Academic Affiliation, Fall, 1–15.

Bradley, R.S., Jonest, P.D., 1993. Little Ice Age summer temperature variations: their nature and relevance to recent global warming trends. The Holocene 3, 367–376.

Bryson, R.A., Wendland, W.M., Ives, J.D., Andrews, J.T., 1969. Radiocarbon isochrones on the disintegration of the Laurentide ice sheet. Arctic and Alpine Research 1 (1), 1–13.

Chauhan, M.S., Kumar, K., Quamar, M.F., Sharma, A., 2013. Correlation of data on loss-on-ignition and palynology for Late Quaternary climate change in southwestern Madhya Pradesh, India. Current Science 104 (3), 299–301.

Ding, X., Bassinot, F., Guichard, F., Fang, N.Q., 2013. Indonesian through flow and monsoon activity record in The Timor Sea since the last glacial maximum. Marine Micropalaeontology 101, 115–126.

Dypvik, H., Harris, N.B., 2001. Geochemical facies analysis of fine-grained siliciclastic using Th/U, Zr/Rb and (Zr+Rb)/Sr ratios. Chemical Geology 181, 131–146.

Easterbrook, D.J., 2016. Temperature fluctuations in Greenland and the Arctic. In: Easterbrook, D.J. (Ed.), Evidence – Based Climate Science – Data Opposing CO_2 Emissions as the Primary Source of Global Warming, 137–160, ScienceDirect.

Ellison, C.R.W., Chapman, M.R., Hall, I.R., 2006. Surface and deep ocean interactions during the cold climate event 8200 years ago. Science 312, 1929–1932.

Effendi, A.C., Apandi, C., 1993. Simplified Geological Map of Sumba Quadrangle, Nusa Tenggara, Scale 1:250.000. Report of Geolocal Research and Development Centre, Bandung, Indonesia.

Gagan, M.K., Ayliffe, L.K., Hopley, D., Cali, J.A., Mortimer, G.E., Chappell, J., McCulloch, M.T., Head, M.J., 1998. Temperature and surface-ocean water balance of the Mid-Holocene tropical Western Pacific. Science 279, 1014–1018.

Gagan, M.K., Ayliffe, L.K., Beck, J.W., Cole, J.E., Druffel, E.R.M., Dunbar, R.B., Schrag, D.P., 2000. New views of tropical palaeoclimates from corals, Quaternary Science Reviews 19 (1–5), 45–64.

Griffiths, M.L., Drysdale, R.N., Gagan, M.K., Zhao, J., Ayliffe, L.K., Hellstrom, J.C., Hantoro, W.S., Frisia, S., Feng, Y., Cartwright, I., St. Pierre, E., Fischer, M.J., Suwargadi, B.W., 2009. Increasing Australian-Indonesian monsoon rainfall linked to early Holocene sea-level rise. Nature Geoscience 2, 636–639.

Griffiths, M.L., Drysdale, R.N., Gagan, M.K., Frisia, S., Zhao, J.-X., Ayliffe, L.K., Hantoro, W.S., Hellstrom, J.C., Fischer, M.J., Feng, Y.-X., Suwargadi, B.W., 2010. Evidence for Holocene changes in Australian-Indonesian monsoon rainfall from stalagmite trace element and stable isotope ratios. Earth and Planetary Science Letters 292, 27–38.

Gustiantini, L., 2018. Palaeoclimate reconstructions by multiproxy approaches in Halmahera Sea since the Late Pleistocene–Holocene. Doctoral Program Dissertation, Institut Teknologi Bandung, 79–86.

Hemming, S.R., 2007. Terrigenous sediments, Palaeoceanography, Physical and Chemical Proxies. Elsevier B.V., 1776–1786.

IPCC., 2012. Summary for Policymakers. In: Managing the Risks of Extreme Events and Disasters to Advance Climate Change Adaptation [Field, C.B., V.R. Barros, T.F. Stocker, D. Qin, D.J. Dokken, K.L. Ebi, M.D. Mastrandrea, K.J. Mach, G.-K. Plattner, S.K. Allen, M. Tignor, and P.M. Midgley (eds.)]. Cambridge University Press, Cambridge, United Kingdom and New York, NY, USA, 3–21.

IPCC., 2013. Principles Governing IPCC Work. Intergovernmental Panel on Climate Change (IPCC), Geneva, Switzerland, 2 pp.

IPCC., 2014. Summary for Policymakers. In: Climate Change 2014: Impacts, Adaptation, and Vulnerability. Part A: Global and Sectoral Aspects. Contribution of Working Group II to the Fifth Assessment Report of the Intergovernmental Panel on Climate Change [Field, C.B., V.R. Barros, D.J. Dokken, K.J. Mach, M.D. Mastrandrea, T.E. Bilir, M. Chatterjee, K.L. Ebi, Y.O. Estrada, R.C. Genova, B. Girma, E.S. Kissel, A.N. Levy, S. MacCracken, P.R. Mastrandrea, and L.L. White (eds.)]. Cambridge University Press, Cambridge, United Kingdom and New York, NY, USA, pp. 1–32.

IPCC., 2017. Meeting Report of the Intergovernmental Panel on Climate Change Expert Meeting on Mitigation, Sustainability and Climate Stabilization Scenarios. [Shukla, P.R., J. Skea, R. Diemen, E. Huntley, M. Pathak, J. PortugalPereira, J. Scull, and R. Slade (eds.)]. IPCC Working Group III Technical Support Unit, Imperial College London, London, UK, 44 pp.

Keigwin, L.D., 1996. The Little Ice Age and Medieval Warm Period in the Sargasso Sea. Science 274, 1504–1508.

Kissel, C., Laj, C., Kienast, M., Bolliet, T., Holbourn, A., Hill, P., Kuhnt, W., Braconnot, P., 2010. Monsoon variability and deep oceanic circulation in the western equatorial Pacific over the last climatic cycle: Insights from sedimentary magnetic properties and sortable silt. Palaeoceanography 25, 1–12.

Kuhnert, H., Kuhlmann, H., Mohtadi, M., Meggers, H., Baumann, K.-H., Patzold, J., 2014. Holocene tropical western Indian Ocean sea surface temperatures in covariation with climatic changes in the Indonesian region. Palaeoceanography 29, 423–437.

Langer, M.R., 2008. Assesing the contribution of foraminiferan protists to global ocean carbonate production. Journal of Eukaryotic Microbiology 55 (3), 163–169.

Linsley, B.K., Rosenthal, Y., Oppo, D.W., 2010. Holocene evolution of the Indonesian throughflow and the western Pacific warm pool. Nature Geosceince 3, 578–583.

Liu, E., Wang, X.-C., Zhao, J.-X., Wang, X., 2015. Geochemical and Sr-Nd isotopic variations in a deep-sea sediment core from Eastern Indian Ocean: Constraints on dust provenances, palaeoclimate and volcanic eruption history in the last 300,000 years. Marine Geology 367, 38–49.

Lytwyn, J., Rutherford, E., Burke, E., Xia, C., 2001. The geochemistry of volcanic, plutonic and turbiditic rocks from Sumba, Indonesia. Journal of Asian Earth Sciences 19 (4), 481–500.

Mayewski, P.A., Rohling, E.E., Stager, J.C., Karlen, W., Maasch, K.A., Meeker, L.D., Meyerson, E.A., Gasse, F., van Kreveld, S., Holmgren, K., Lee-Thorp, J., Rosqvist, G., Rack, F., Staubwasser, M., Schneider, R.R., Steig, E.J., 2004. Holocene climate variability. Quaternary Research 62 (3), 243–355.

Maxwell, A.L., 1999. Holocene environmental change in Mainland Southeast Asia: Pollen and charcoal records from Cambodia. PhD Thesis, Louisiana State University.

Mohtadi, M., Oppo, D.W., Steinke, S., Stuut, J.-B.W., De Pol-Holz, R., Hebbeln, D., Lückge, A., 2011. Glacial to Holocene swings of the Australian-Indonesian monsoon. Nature Geoscience 4, 540–544.

Park, J., Park, J., Yi, S., Kim, J.C., Lee, E., Choi, J. 2019. Abrupt Holocene climate shifts in coastal East Asia, including the 8.2 ka, 4.2 ka, and 2.8 ka BP events, and societal responses on the Korean Peninsula. Scientific Reports 9:10806 https://doi.org/10.1038/s41598-019-47264-8.

Robertson, S., 2011. Direct estimation of organic matter by loss on ignition methods. http://www.sfu.ca/soils/lab_documents/Estimation_Of_Organic_Matter_By_LOI.pdf.

Ruddiman, W.F., Mix, A.C., 1993. The north and equatorial Atlantic at 9000 and 6000 yr BP. In: Wright, H.E. (Ed.), Global Climates since the Last Glacial Maximum, 94–124. University of Minnesota Press, Minneapolis.

Saraswat, R., 2015. Non-destructive foraminiferal palaeoclimatic proxies: a brief insight. Proceedings Indian National Science Academy 81, 381–395.

Setiabudi, D. A., 1985. Comparaison isotopique a haute resolution decarrotes marines prelevees dans l'arc Indonesien, Memoire du D.E.A de Geologie et Geochemie Sedimentaires. Universite deq Paris-Sud (Unpublished), 77 pp.

Steinke, S., Mohtadi, M., Prange, M., Varma, V., Pittauerova, D., Fischer, H.W., 2014. Mid- to Late Holocene Australian-Indonesian summer monsoon variability. Quaternary Science Reviews 93, 142–154.

Sijinkumar, A.V., Nath, B.N., 2012. Planktic foraminifera: A potential proxy for palaeoclimatic / palaeooceanographic studies. GCK Science Letters 1, 22–30.

Thompson, L.G., Mosley-Thompson, E., Davis, M.E., Lin, P.-N., Henderson, K.A., Cole-Dai, J., Bolzan, J.F., Liu, K.-B., 1995. Late glacial stage and Holocene tropical ice core records from Huascaran, Peru. Science 269, 46–50.

Walker, M., Gibbard, P., Head, M.J., Berkelhammer, M., Bjorck, S., Cheng, H., Cwynar, L.C., Fisher, D., Gkinis, V., Long, A., Lowe, J., Newnham, R., Rasmussen, S.O., Weiss, H. 2019. Formal subdivison of the Holocene Series/Epoch: A summary. Journal of Geological Society of India 93, 135–141.

Watanabe, T., Gagan, M.K., Correge, T., Scott-Gagan, H., Cowley, J., Hantoro, W.S., 2003. Oxygen isotope systematics in *Diploastrea heliopora*: new coral archive of tropical palaeoclimate. Geochemica et Cosmochimica Acta 67 (7), 1349–1358.

Weltje, G.J., Tjallingii, R. 2008. Calibration of XRF core scanners for quantitative geochemical logging of sediment cores: Theory and application. Earth and Planetary Science Letters 274, 423–438.

Yulianto, E., 2001. Holocene climate change based on spectrum analysis of pollen and their implications on tectonic in Sunda Shelf. Master Thesis, Institut Teknologi Bandung (in Indonesian with English summary).